Magnetic phase diagram of metallic pyrochlore lattice in the double-exchange model

Daisaku Ikoma,[1] Hiroki Tsuchiura,[1,2] and Jun-ichiro Inoue[1]
[1]*Department of Applied Physics, Nagoya University, Nagoya 464-8603, Japan*
[2]*International School for Advanced Studies (SISSA), Via Beirut 2-4, 34014, Trieste, Italy*
(Received 27 March 2003; published 16 July 2003)

The magnetic phase diagram of metallic *kagomé* and pyrochlore lattices at the ground state have been studied theoretically in the double-exchange model using a mean-field approximation. The model includes the hopping of itinerant electrons, which is expressed by a single tight-binding band, antiferromagnetic coupling between localized spins, and ferromagnetic exchange interaction between the localized and itinerant electron spins. The phase diagram was found to be rather insensitive to the ferromagnetic exchange interaction but to show a rich variety in magnetic structure with doping. A crossover between ferromagnetic and spin glass phases observed in $RE_2Mo_2O_7$ pyrochlore lattices, where RE denotes rare-earth ions, is discussed in view of the calculated results.

DOI: 10.1103/PhysRevB.68.014420 PACS number(s): 75.25.+z, 71.20.Lp, 75.10.Lp

I. INTRODUCTION

The pyrochlore lattice has recently attracted much attention as a geometrically frustrated magnetic system.[1–3] Many theoretical works have examined the frustrated magnetism of, for example, spin liquid, spin ice, etc., for the pyrochlore lattice and *kagomé* lattice. The latter, a two-dimensional version of the frustrated lattice, is realized on the cross section of the (111) direction of the ideal pyrochlore lattice.[4–11] In addition to study of the localized spin systems, both experimental and theoretical interest has extended to frustrated lattices with metallic characters such as $Tl_2Mn_2O_7$,[12–14] and $RE_2Mo_2O_7$ (RE: rare-earth elements).[15–21]

$Tl_2Mn_2O_7$, a coupled system of localized spins and itinerant electrons with low density, shows the so-called colossal magnetoresistance. In $RE_2Mo_2O_7$, a transition between spin glass and metallic ferromagnetism has been reported, and is explained in terms of the ionic radius of RE elements.[17] An enhancement of the anomalous Hall resistivity at low temperatures in $RE_2Mo_2O_7$ (Refs. 16 and 19) has been explained in terms of the concept of a Berry phase caused by canted spins on the background.[18] Thus the coupling between the localized spins and itinerant electrons gives rise to an interesting phenomenon. It has been suggested[17] that the magnetic properties caused by the coupling between the localized spins and itinerant electrons in $RE_2Mo_2O_7$ may be explained in terms of the so-called double-exchange model.[22–25] Thus far, the magnetic properties of manganites, the typical double-exchange system, have been intensively studied,[26–28] and those of pyrochlore lattices much less so. Because of the geometrical frustration, interesting magnetic phases may also be expected in the metallic pyrochlore lattices. In this work, we will present, as a first step, a mean-fields study on the magnetic phase diagram at the ground state of the pyrochlore and *kagomé* lattices.

The outline of this paper is as follows. In the next section, we introduce the model and method used in this work. The calculated results for *kagomé* and pyrochlore lattices are presented in Sec. III. In that same section, we discuss the possible relevance of those calculated results to experimental results on the transition between spin glass and metallic ferromagnetism observed in $RE_2Mo_2O_7$. In Sec. IV, we argue the effects of electric phase separation and transversal spin fluctuations neglected in the mean-field treatment, and then give a summary.

II. MODEL HAMILTONIAN AND METHOD

We adopt a model in which itinerant electrons and localized spins coexist. The model is clearly applicable to pyrochlore manganites, wherein the localized spins are carried by Mn ions and the itinerant electrons are supplied from the *s* band of Tl ions. The model may also be applicable to $RE_2Mo_2O_7$, in which the localized spins reside on RE ions or possibly on Mo *d* levels and the itinerant electrons are supplied from *d* states of Mo ions.

Hereafter, we treat the itinerant electrons in a single orbital tight-binding model, in which they interact with the localized spins via a ferromagnetic exchange coupling (Hund coupling). We also include antiferromagnetic superexchange interaction between localized spins. The spin angular momentum of the localized spins is taken to be *S*.

The Hamiltonian of the model is given as

$$H = t\sum_{ij\sigma} c_{i\sigma}^{\dagger} c_{j\sigma} - K\sum_{i} \mathbf{s}_i \cdot \mathbf{S}_i + J\sum_{\langle ij \rangle} \mathbf{S}_i \cdot \mathbf{S}_j . \qquad (1)$$

The first term represents the hopping of electrons with spin σ between nearest neighbor (NN) sites *i* and *j*, with overlap integral *t*. The second term represents a ferromagnetic exchange interaction (i.e., the Hund coupling) between itinerant electron spin $\mathbf{s}_i$ and localized spin $\mathbf{S}_i$ at site *i*, where *K* stands for the coupling constant. The last term denotes an antiferromagnetic exchange interaction between localized spins that occurs between NN sites with a coupling constant *J*.

We concentrate on the magnetic phase diagram at the ground state (GS) and apply a mean-field approximation to both ferromagnetic and antiferromagnetic exchange interactions given in Eq. (1). In the approximation, the antiferromagnetic interaction represents an energy that depends on

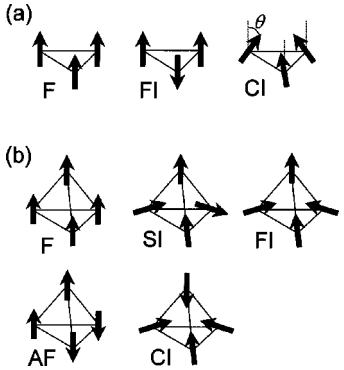

FIG. 1. Types of spin configuration for (a) *kagomé* lattice and (b) pyrochlore lattice.

the relative angle of localized spins, and the Hund coupling gives an effective field acting on the itinerant electrons. The electronic states of the itinerant electrons are calculated by taking into account the effective field in the unit cell, which is composed by three atomic sites in the *kagomé* lattice and by four atomic sites in the pyrochlore lattice. The GS is determined by comparing the energy for various spin configurations within the unit cell.

The types of spin configurations for the *kagomé* lattice are shown in Fig. 1(a). Herein, they are called ferromagnetic (F), ferrimagnetic (FI), and chiral (CI) spin configurations. Those for the pyrochlore lattice are shown in Fig. 1(b); they are called the ferromagnetic (F), antiferromagnetic (AF), ferrimagnetic (FI), chiral (CI), spin and spin ice (SI) configurations. In the chiral spin configurations, the canted angle θ is adjusted to realize the lowest energy state.

In the next section, phase diagrams are depicted in a space of K and electron number n per unit cell (u.c.) for several values of J. We hereafter take the hopping integral t as the energy unit. The order of J will be estimated later from the magnetic transition temperatures observed.

III. CALCULATED RESULTS

A. *Kagomé* lattice

A phase diagram in $K-n$ space for $J/t=0$ is shown in Fig. 2(a). Here the electron number n varies from 0 to 6, including both spins based on the fact that the u.c. contains three atoms. We find that the GS is rather independent of the value of K, but depends on n. Because $J=0$, the kinetic motion of electrons gives rise to an energy gain, and therefore the F state is favorable as the GS. The F state is actually realized for $n \lesssim 2$ and $n \gtrsim 4$, as shown in Fig. 2(b), whereas the CI state is stable for the highly doped region. There are two possible explanations: one is that a superexchange interaction is realized near half filled states as is usually observed in strongly correlated electron systems; the other is that an effective antiferromagnetic interaction is induced as a result of band-structure effect—that is, the magnetic susceptibility $\chi(Q)$ shows a maximum value for a nonzero wave vector when the Fermi level is located near the band center.

The FI state is realized at the boundary between the F and CI states near $n \sim 4$. The physical explanation of this result is

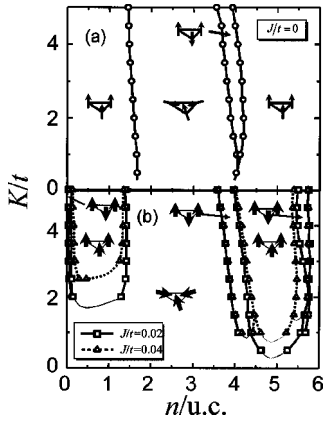

FIG. 2. (a) Calculated phase diagram for *kagomé* lattice for $J/t=0$ and (b) $J/t=0.02$ (squares) and 0.04 (triangles). Lines are guide for the eye.

rather difficult to convey, but it might be caused by a shape of the density of states (DOS). It is well known that the DOS of the *kagomé* lattice contains a δ-function-type of state at one of the band edges. The position of the δ-function-type DOS is determined by the sign of the hopping integral t. In the present case, we have chosen the sign of t in such a way that it appears at the top of the band. Because the δ function type of DOS contains two electrons, including both spins, the Fermi level is located at a DOS of strong energy dependence when $n \sim 4$. The complex shape of the DOS may be a possible reason for the occurrence of the FI state for $n \sim 4$.

Figure 2(b) shows the calculated results of the phase diagram for the *kagomé* lattice with $J/t=0.02$ and 0.04. We find that the CI state stabilizes in the region of small K and in those with $n \sim 0$ and ~ 6. When K is small, the AF interaction dominates over the ferromagnetic Hund coupling, and the CI state becomes stable. The thin solid and the broken curves show an interpolation of the calculated points represented by symbols. At low electron and hole-doped regions, the kinetic energy gain is not sufficient to overcome the AF interaction between localized spins, and the CI state therefore becomes stable.

A phase diagram in $K-J$ space is shown in Fig. 3 for $n=1.0$. When K is large, the F state is realized, the CI state is realized when J is large. The result may be easily understood without detailed explanation.

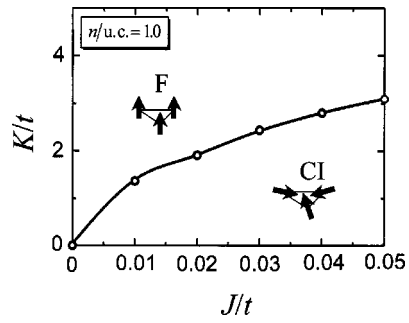

FIG. 3. A $K-J$ phase diagram of the ground state of a *kagomé* lattice with $n=1.0$ per unit cell.

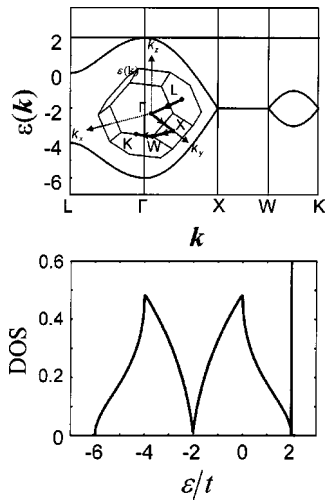

FIG. 4. (a) Energy dispersion ($E(\mathbf{k})$) and (b) density of states (DOS) of a pyrochlore lattice without interaction.

B. Pyrochlore lattice

We first show the energy dispersion $E(\mathbf{k})$ and DOS of the pyrochlore lattice without interaction terms, in Figs. 4(a) and (b), respectively. We have chosen the sign of t to be negative so that a δ-function-type DOS is located at the top of the band. The δ-function-type state is doubly degenerate.

Figures 5(a) and (b) are the DOS for the CI and AF states, respectively, with $J/t=0$, $K/t=4.0$, and $n=4.0$ per u.c. The shape of the DOS near the top of the band is strongly modified to give complex structures for both cases. The Fermi level in these cases is located near the lower edge of the complex DOS.

The calculated phase diagram in $K-n$ space for $J/t=0$ is presented in Fig. 6(a). We find that the magnetic phase is rather independent of the value of K/t, as in the *kagomé* lattice. The F state appears in the low electron-and hole-doped regions, and the AF state is realized near half filling. The reason for the AF state may also be the instability of $\chi(Q)$ with nonzero Q, as explained for the *kagomé* lattice. The reason for the stability of the CI state in a region of $2.0 \lesssim n \lesssim 4.0$ may be the same as that for the stability of the AF state; that is, a band structure effect on $\chi(Q)$. A discontinuity of the boundary between the CI and AF states near

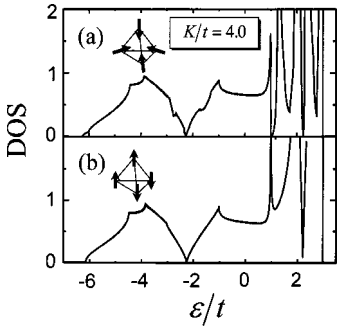

FIG. 5. Densities of states of pyrochlore lattice for $K/t=4.0$, $J/t=0$, and $n=4.0$ per unit cell, (a) CI and (b) AF spin configuration.

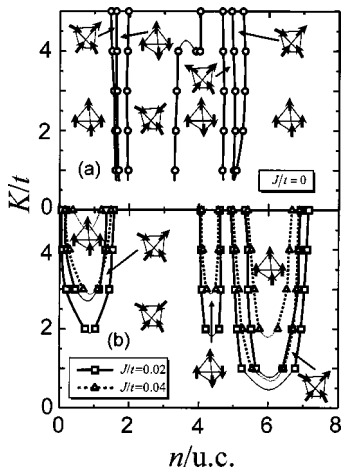

FIG. 6. $K-n$ phase diagram at the ground state for a pyrochlore lattice with (a) $J/t=0$, and (b) $J/t=0.02$ and 0.04. When $J/t=0$, the magnetic structure varies relative to F/FI/AF/CI/AF/SI/FI/F with increasing n.

$K/t=4.0$ may be due to an effect of the complex shape of DOS, based on the fact that the Fermi level touches a peak of DOS for both states, as can be seen in Figs. 5(a) and (b). The boundary, however, should be continuous, though it was not confirmed. The FI and SI states appear between the F and CI states, and between the F and AF states, respectively, as an intermediate state.

Figure 6(b) shows the phase diagrams for $J/t=0.02$ and 0.04. It is seen that both the F and AF state shrink and the CI state extends over a wide region. The shrinkage of the F and AF states and extension of the CI state can be easily understood because the exchange energy between localized spins are $3J$, $-J$, and $-3J/2$ per u.c. for the F, AF, and CI (with canting angle $\theta=0.5\pi$) states, respectively. The CI state with the lowest exchange energy extends over a wide region with increasing J. The FI state, the exchange energy of which is 0, appears at the boundaries between F and CI states as a crossover state. The SI state disappears with increasing J because its exchange energy is $J/2$ per u.c.

The phase diagram in $K-J$ space is shown in Fig. 7 for $n=1.0$ per u.c. As expected, the F state is stable when K/t is large, whereas the CI state is stable when J/t is large. The FI state appears as an intermediate state. In order to make a comparison between theoretical and experimental results, we should further study the energy dependence on the t because

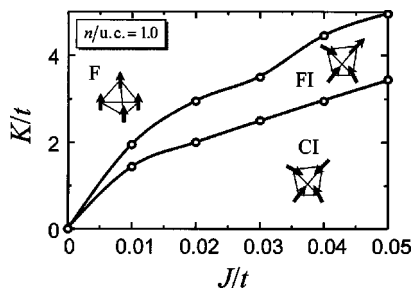

FIG. 7. $K-J$ phase diagram at $n=1.0$ per unit cell for a pyrochlore lattice.

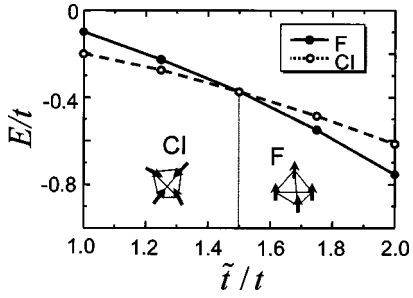

FIG. 8. Comparison of the ground-state energy between CI and F spin configurations as functions of hopping integral.

the phase diagram in $K/t-J/t$ space may not give correct information on t dependence of the magnetic state. This is because the kinetic energy of itinerant electrons is influenced by K and t independently. The comparison between theoretical and experimental results will be presented in the next subsection.

C. Comparison with the experimental results

In $RE_2Mo_2O_7$, a crossover from F to the spin-glass phase appears with decreasing the ionic radius of RE ions; that is, with decreasing the hopping integral between Mo ions.[17] This is attributed to a change in the angle of the Mo-O-Mo bond. It is well known that in manganites, the magnetic state is dependent on the angle of the Mn-O-Mn bond. Because the kinetic energy includes both K and t as independent parameters, the phase diagram shown in Fig. 7 may not give an explanation of the crossover caused by the bond angle. Therefore we performed an energy calculation by changing the value of t for the CI and F states.

Taking into account the experimental situation for $RE_2Mo_2O_7$, we chose the parameter values in the following way. The number of electrons in $Sm_2Mo_2O_7$ was reported to be ~ 0.4/Mo ion by the Hall resistivity.[16] Because $RE_2Mo_2O_7$ forms a double pyrochlore lattice structure for RE and Mo ions, the average number per unit cell per orbital may be considered to be 0.16. Therefore we assumed $n=0.1$ per unit cell. The values of the hopping integral t were estimated to be 0.09 eV by using realistic tight-binding parameter values.[29] With $S=\frac{1}{2}$ for both cases, the values of K/t and J/t were determined to be 2.0 and 0.04, respectively. The former value gives 25 K for the ferromagnetic Curie temperature in the mean-field approximation, and the latter gives 8 K for the spin-glass transition temperature in a cluster mean-field approximation.[11] These transition temperatures may be low compared with those for $T_C \sim 70$ K and $T_{SG} \sim 20$ K, though, when we take $S=1$, higher transition temperatures may be obtained.

Figure 8 shows the calculated results of the total energy of the CI and F states. We see that the F state becomes unstable when the hopping integral becomes smaller; that is, with decreasing the bond angle. The result agrees qualitatively with the results of experiments. The actual change in the bond angle is small, and gives only a 2% change in t. Although a detailed study is required to make a quantitative argument, it is interesting to note that the energy difference between F and CI states within this narrow window of t is at most 10^{-3} eV, which corresponds to a few tens of tesla for the external magnetic field.

IV. DISCUSSION

In an energy diagram designed to find the lowest energy state as a function of n, we find that a common tangential line between neighboring states can be drawn. This indicates that an electric phase separation[26] may occur near the phase boundaries shown in the phase diagrams. Therefore the fine structures near the boundaries may be washed away, and, instead, coexisting regions with different respective magnetic phases may appear. A detailed energy comparison between magnetic states at low electron density revealed that the dependence of the energy on n is convex upwards; consequently the electronic phase separation also occurs in the low electron density region. We expect that only the F and CI states survive in the *kagomé* lattice, and the F, AF, CI states remain in the pyrochlore lattice.

We adopted the mean-field approximation, which may be sufficiently valid when the interactions in the Hamiltonian are relatively weak as compared to the hopping parameter of the electrons. It may be necessary, however, to check the validity of this method by comparing the results to those obtained in an improved approximation, given that the value of K is rather large relative to t. Here we study the effects of local spin fluctuations on the electronic state of a single electron in the antiferromagnetic spin ordering for the pyrochlore lattice. The Hamiltonians for the ferromagnetic and antiferromagnetic couplings, H_K and H_J in Eq. (1), are given as

$$H_K=-\frac{1}{2}K\sum_i\ [(c_{i\uparrow}^{\dagger}c_{i\uparrow}-c_{i\downarrow}^{\dagger}c_{i\downarrow})S_i^Z+c_{i\uparrow}^{\dagger}c_{i\downarrow}S_i^-+c_{i\downarrow}^{\dagger}c_{i\uparrow}S_i^+], \tag{2}$$

$$H_J=J\sum_{\langle ij\rangle}\left[S_i^ZS_j^Z+\frac{1}{2}(S_i^+S_j^-+S_i^-S_j^+)\right], \tag{3}$$

respectively. The itinerant electron interacts with the localized spins within the unit cell and causes spin flip, which may further result in excitation of localized spins due to exchange coupling via the J term. By choosing a suitable variational function, which includes possible spin configurations within the unit cell, we can describe the motion of a single electron introduced in the AF state.[30] Hereafter, we take $S=\frac{1}{2}$, and restrict the spin flip of the localized spins within the unit cell where the itinerant electron is located. Due to the translational invariance of the lattice, we are able to construct the Bloch functions using the variational function.

By comparing the calculated results of the energy dispersions with the $E(\mathbf{k})$ shown in Fig. 4(a), we find that there is almost no modification of $E(\mathbf{k})$ in the low-energy region. Strong disturbance may appear in the energy region of K/t, measured from the bottom of the band. The results indicate that the transversal component of the Hamiltonian may not give strong effects on the electronic states of the itinerant electrons so long as the number of electrons is small. Further

investigation, however, may be warranted, given that the effects of long-range spin fluctuations were examined in the present treatment.

V. SUMMARY

Phase diagrams of the magnetic states have been studied for geometrically frustrated lattices, including *kagomé* and pyrochlore lattices, by using the double-exchange model with an AF exchange interaction between localized spins. When the AF interaction J/t is small, the magnetic states are rather insensitive to K/t and dependent on the number of itinerant electrons. Ferromagnetic spin ordering appears in the low electron (hole) density regions as a result of gain in the kinetic energy of electrons, whereas antiferromagnetic or chiral spin ordering is stable near half filling, which may be due to band effects. With increasing J/t, the chiral spin state is stabilized in the pyrochlore lattice. Near the phase boundary between the ferromagnetic and chiral or antiferromagnetic states, however, an electric phase separation has been suggested to occur. The crossover between the ferromagnetic and spin glass phases observed in Mo oxides with a pyrochlore lattice has been explained qualitatively by introducing a change in the hopping integral caused by the bending of Mo-O-Mo bonds. The present study may be a good starting point from which to study geometrically frustrated lattices such as $RE_2Mo_2O_7$ in order to understand their basic properties.

ACKNOWLEDGMENTS

J.I. is thankful for financial support from the CREST, JST, Japan, the NEDO international joint project ''Nano-scale magnetoelectronics;'' and for a Grant-in-Aid for Scientific Research (C) of the Ministry of Education, Culture, Sports, Science and Technology of Japan.

[1] A. P. Ramirez, A. Hayashi, R. J. Cava, R. Siddharthan, and B. S. Shastry, Nature (London) **399**, 333 (1999).
[2] J. S. Gardner, B. D. Gaulin, S.-H. Lee, C. Broholm, N. P. Raju, and J. E. Greedan, Phys. Rev. Lett. **83**, 211 (1999).
[3] A. P. Ramirez, *Handbook of Magnetic Materials*, edited by K. H. J. Buschow (Elsevier Science, North-Holland, 2001), Vol. 13, p. 423.
[4] J. N. Reimers, A. J. Berlinsky, and A.-C. Shi, Phys. Rev. B **43**, 865 (1991).
[5] R. R. P. Singh and D. A. Huse, Phys. Rev. Lett. **68**, 1766 (1992).
[6] M. J. Harris, S. T. Bramwell, D. F. Mcmorrow, T. Zeiske, and K. W. Godfrey, Phys. Rev. Lett. **79**, 2554 (1997).
[7] R. Moessner and J. T. Chalker, Phys. Rev. Lett. **80**, 2929 (1998).
[8] B. Canals and C. Lacroix, Phys. Rev. Lett. **80**, 2933 (1998).
[9] M. J. Harris, S. T. Bramwell, P. C. W. Holdsworth, and J. D. M. Champion, Phys. Rev. Lett. **81**, 4496 (1998).
[10] P. Sindzingre, G. Misguich, C. Lhuillier, B. Bernu, L. Pierre, C. Waldtman, and H.-U. Everts, Phys. Rev. Lett. **84**, 2953 (2000).
[11] A. J. Garcia-Adeva and D. L. Huber, Phys. Rev. Lett. **85**, 4598 (2000).
[12] Y. Shimakawa, Y. Kubo, and T. Manako, Nature (London) **379**, 53 (1996).
[13] M. A. Subramanian, B. H. Toby, A. P. Ramirez, W. J. Marchall, A. W. Sleight, and G. H. Kwei, Science **273**, 81 (1996).
[14] S.-H. Cheong, H. Y. Hwang, B. Batlogg, and L. W. Rupp, Jr., Solid State Commun. **98**, 163 (1996).
[15] B. Martinez, R. Senis, J. Fontcuberta, X. Obradors, W. Cheikh-Rouhou, P. Strobel, C. Bougerol-Chaillout, and M. Pernet, Phys. Rev. Lett. **83**, 2022 (1999).
[16] Y. Taguchi and Y. Tokura, Phys. Rev. B **60**, 10 280 (1999).
[17] T. Katsufuji, H. Y. Hwang, and S-W. Cheong, Phys. Rev. Lett. **84**, 1998 (2000).
[18] K. Ohgushi, S. Murakami, and N. Nagaosa, Phys. Rev. B **62**, R6065 (2000).
[19] Y. Taguchi, Y. Oohara, H. Yoshizawa, N. Nagaosa, and Y. Tokura, Science **291**, 2573 (2001).
[20] S. Iikubo, S. Yoshii, T. Kageyama, K. Oda, Y. Kondo, K. Murata, and M. Sato, J. Phys. Soc. Jpn. **70**, 212 (2001).
[21] S. Yoshii, S. Iikubo, T. Kageyama, K. Oda, Y. Kondo, K. Murata, and M. Sato, J. Phys. Soc. Jpn. **69**, 3773 (2000).
[22] C. Zener, Phys. Rev. **82**, 403 (1951).
[23] P. W. Anderson and H. Hasegawa, Phys. Rev. **100**, 675 (1955).
[24] P.-G. de Gennes, Phys. Rev. **118**, 141 (1960).
[25] J. Inoue and S. Maekawa, Phys. Rev. Lett. **74**, 3407 (1995).
[26] A. Moreo, S. Yunoki, and E. Dagotto, Science **283**, 2034 (1999).
[27] T. Ohsawa and J. Inoue, Phys. Rev. B **65**, 014401 (2002).
[28] T. Ohsawa and J. Inoue, Phys. Rev. B **65**, 134442 (2002).
[29] W. A. Harrison, *Electronic Structure and the Properties of Solids* (Dover Publications, New York, 1980).
[30] S. Akazawa, J. Inoue, and S. Maekawa, J. Phys. Soc. Jpn. **66**, 2758 (1997).